

## Iron PCP Pincer Complexes in Three Oxidation States: Reversible Ligand Protonation To Afford an Fe(0) Complex with an Agostic C–H Arene Bond

Daniel Himmelbauer,<sup>†</sup> Matthias Mastalir,<sup>†</sup> Berthold Stöger,<sup>‡</sup> Luis F. Veiros,<sup>§</sup> Marc Pignitter,<sup>||</sup> Veronika Somoza,<sup>||</sup> and Karl Kirchner<sup>\*,†</sup>

<sup>†</sup>Institute of Applied Synthetic Chemistry, Vienna University of Technology, Getreidemarkt 9, A-1060 Vienna, Austria

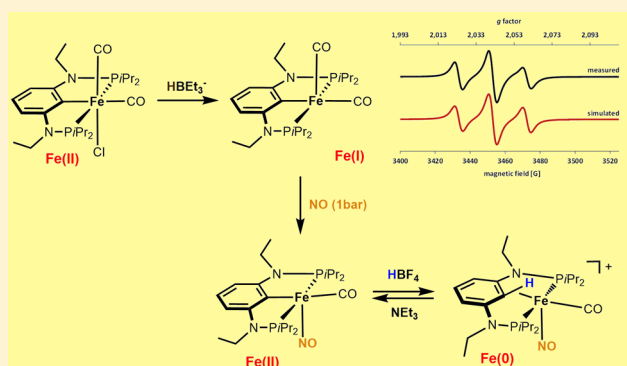
<sup>‡</sup>X-Ray Center, Vienna University of Technology, Getreidemarkt 9, A-1060 Vienna, Austria

<sup>§</sup>Centro de Química Estrutural, Instituto Superior Técnico, Universidade de Lisboa, Av. Rovisco Pais No. 1, 1049-001 Lisboa, Portugal

<sup>||</sup>Department of Physiological Chemistry, Faculty of Chemistry, University of Vienna, Althanstrasse 14, 1090 Vienna, Austria

### Supporting Information

**ABSTRACT:** In the current investigation, the reaction of  $\text{Fe}_2(\text{CO})_9$  with the ligand precursor 2-chloro- $N^1,N^3$ -bis(diisopropylphosphanyl)- $N^1,N^3$ -diethylbenzene-1,3-diamine ( $\text{P}(\text{C}-\text{Cl})\text{P}^{\text{NEt}}-i\text{Pr}$ ) (**1**) was investigated. When a suspension of  $\text{Fe}_2(\text{CO})_9$  and **1** in  $\text{CH}_3\text{CN}$  was transferred in a sealed microwave glass vial and stirred for 18 h at 110 °C the complex  $[\text{Fe}(\text{PCP}^{\text{NEt}}-i\text{Pr})(\text{CO})_2\text{Cl}]$  (**2**) was obtained. In an attempt to prepare the hydride Fe(II) complex  $[\text{Fe}(\text{PCP}^{\text{NEt}}-i\text{Pr})(\text{CO})_2\text{H}]$  (**3**), **2** was reacted with 1 equiv of  $\text{Li}[\text{HBEt}_3]$  in THF. Instead of ligand substitution, this complex underwent a one electron reduction which led to the formation of the low-spin  $d^7$  Fe(I) complex  $[\text{Fe}(\text{PCP}^{\text{NEt}}-i\text{Pr})(\text{CO})_2]$  (**4**). Exposure of a benzene solution of **4** to NO gas (1 bar) at room temperature affords the diamagnetic complex  $[\text{Fe}(\text{PCP}^{\text{NEt}}-i\text{Pr})(\text{CO})(\text{NO})]$  (**5**). This is the first iron PCP nitrosyl complex. Protonation of **5** with  $\text{HBF}_4 \cdot \text{Et}_2\text{O}$  affords the cationic Fe(0) complex  $[\text{Fe}(\kappa^3\text{P}, \text{CH}_2\text{P}-\text{P}(\text{CH})\text{P}^{\text{NEt}}-i\text{Pr})(\text{CO})(\text{NO})]\text{BF}_4$  (**6**) which features an  $\eta^2\text{-C}_{\text{aryl}}\text{-H}$  agostic bond. Even with relatively weak bases such as  $\text{NEt}_3$  the agostic C–H bond can be deprotonated with reformation of the starting material **5**. Therefore, protonation of **5** is completely reversible.



## INTRODUCTION

PCP pincer complexes<sup>1</sup> where phosphine donors are connected via  $\text{CH}_2$ , O, or NR spacers to an aromatic benzene backbone in the two ortho positions have received considerable attention over the last decades.<sup>2</sup> This type of compounds can be rationally designed in a modular fashion which permits the preparation of highly active catalysts for a variety of chemical reactions which proceed with high efficiency and selectivity.<sup>2</sup> An established synthetic approach is an intramolecular directed C–H bond coordination to electron rich low-valent metal fragments,<sup>3</sup> followed by oxidative addition of the agostic C–H bond of the  $\text{P}(\text{C}-\text{H})\text{P}$  ligand leading to the generation of (hydride) PCP complexes.

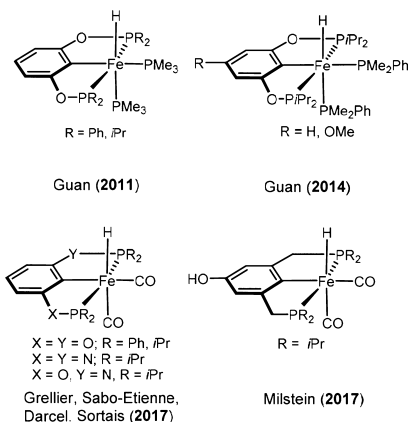
With respect to nonprecious metals, the chemistry of nickel PCP complexes is already quite comprehensive, while studies of cobalt, iron, and molybdenum PCP pincer complexes are exceedingly rare or virtually nonexistent, such as in the case of copper, manganese, chromium, or vanadium.<sup>2p</sup> This may be

attributed to the failure of many simple metal salts to cleave the C–H bonds of the arene moiety of the pincer ligands and/or the thermodynamic instability of the resulting hydride complexes.<sup>4</sup> As iron is concerned, to date, there are only three established systems. Guan and co-workers synthesized the first Fe(II) PCP pincer complexes via a direct cyclometalation route by treatment of the Fe(0) precursor  $\text{Fe}(\text{PMe}_3)_4$  with resorcinol-derived bis(phosphinite) PCP ligand pincer ligands (Chart 1).<sup>5–7</sup> The groups of Sortais<sup>8</sup> and Milstein<sup>9</sup> and co-workers described a new and efficient method based on the commercially available Fe(0) reagent  $\text{Fe}(\text{CO})_5$  for the simple synthesis of well-defined cyclometalated hydride carbonyl PCP iron pincer complexes under mild conditions and UV irradiation.

Here we utilize the oxidative addition of 2-chloro- $N^1,N^3$ -bis(diisopropylphosphanyl)- $N^1,N^3$ -diethylbenzene-1,3-diamine

Received: April 14, 2018

## Chart 1. Examples of Iron PCP Complexes

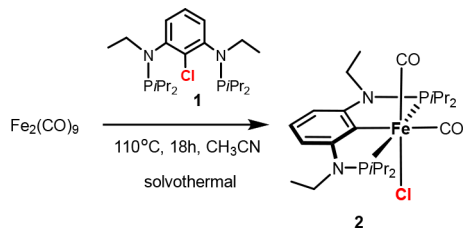


(P(C–Cl)P<sup>NEt</sup>-iPr) (1) to the Fe(0) complex [Fe<sub>2</sub>(CO)<sub>9</sub>] as a synthetic approach for the synthesis of the Fe(II) PCP complex [Fe(PCP<sup>Et</sup>-iPr)(CO)<sub>2</sub>Cl] (2). This complex is a valuable precursor for iron PCP pincer complexes in oxidation states +I and 0. X-ray structures of representative complexes are presented.

## RESULTS AND DISCUSSION

When a suspension of [Fe<sub>2</sub>(CO)<sub>9</sub>] and P(C–Cl)P<sup>NEt</sup>-iPr (1) in acetonitrile was placed in a sealed microwave glass vial and stirred for 18 h at 110 °C, the analytically pure complex [Fe(PCP<sup>NEt</sup>-iPr)(CO)<sub>2</sub>Cl] (2) was obtained in 47% isolated yield (Scheme 1). This complex was fully characterized by a

## Scheme 1. Synthesis of Complex 2



combination of <sup>1</sup>H, <sup>13</sup>C{<sup>1</sup>H}, and <sup>31</sup>P{<sup>1</sup>H} NMR spectroscopy, IR spectroscopy, and HR-MS analysis. In the <sup>13</sup>C{<sup>1</sup>H} NMR spectrum this complex exhibits a characteristic triplet resonance at 137.5 ppm (*J*<sub>PC</sub> = 14.4 Hz) assigned to the *ipso* carbon of the benzene moiety and two low-field triplet resonances at 215.6 and 212.7 ppm assignable to the carbonyl carbon atoms *trans* and *cis* to the *ipso* carbon. Two strong absorption bands typical of a *cis* CO arrangement observed at 2002 and 1934 cm<sup>-1</sup>, respectively, are detected in the IR spectrum. In addition, the solid-state structure of 2 was established by single-crystal X-ray crystallography. A molecular view is depicted in Figure 1 with selected bond distances given in the captions.

We considered this complex as an ideal candidate for the synthesis of a hydride PCP complex. Thus, in an effort to prepare the hydride Fe(II) complex [Fe(PCP<sup>NEt</sup>-iPr)(CO)<sub>2</sub>H] (3), complex 2 was reacted with 1 equiv of Li[HBet<sub>3</sub>] in THF. Instead of ligand substitution, this complex underwent a formal one electron reduction which afforded the Fe(I) complex [Fe(PCP<sup>NEt</sup>-iPr)(CO)<sub>2</sub>] (4) (Scheme 2). It has to be noted that the related pyrrole-based Fe(II) complex [FeCl(py)-

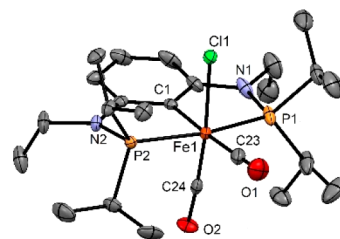
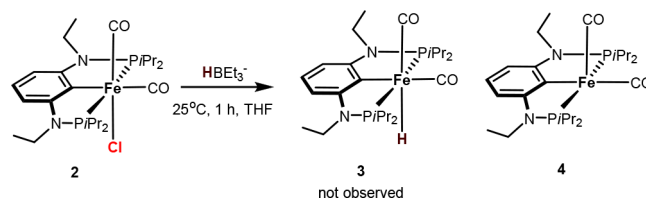


**Figure 1.** Structural view of [Fe(PCP<sup>Et</sup>-iPr)(CO)<sub>2</sub>Cl] (2) showing 50% thermal ellipsoids (H atoms omitted for clarity). Selected bond lengths (Å) and bond angles (deg): Fe1–C1 2.002(2), Fe1–P2 2.2561(7), Fe1–P1 2.270(2), Fe1–Cl1 2.334(2), Fe1–C24 1.713(8), Fe1–C23 1.818(3), P2–Fe1–P1 162.99(5).

## Scheme 2. Synthesis of Complex 4



(C<sup>y</sup>PNP)] reacted with Na[HBet<sub>3</sub>] in the presence of CO to yield the low-spin Fe(I) dicarbonyl complex [Fe(CO)<sub>2</sub>(C<sup>y</sup>PNP)].<sup>10</sup> Complex 4 was isolated in 93% yield as an air-sensitive dark violet solid. As judged by electron paramagnetic resonance (EPR) studies and solution magnetic susceptibility measurements (benzene, Evans method), this compound is a low-spin complex. The solution effective magnetic moment of 1.8(1) μ<sub>B</sub> is in agreement with a low-spin d<sup>7</sup> center (one unpaired electron).

In the X-band EPR spectrum, an isotropic triplet at *g*<sub>iso</sub> = 2.038 with a well-resolved hyperfine coupling to the phosphorus atoms *A* = 19.5 G is observed (Figure 2). Most reported low-spin Fe(I) compounds feature EPR spectra with *g* values close to 2.0.<sup>11</sup>

The frontier orbitals of complex 4 are also typical of a low spin d<sup>7</sup> species with a square pyramidal geometry (Figure 3).<sup>12</sup> The HOMO (single occupied) is based on a metal *z*<sup>2</sup> orbital with a strong component pointing to the empty sixth coordination position, and the LUMO is the Fe–L σ\* orbital involving the *x*<sup>2</sup>–*y*<sup>2</sup> metal orbital, antibonding to all four

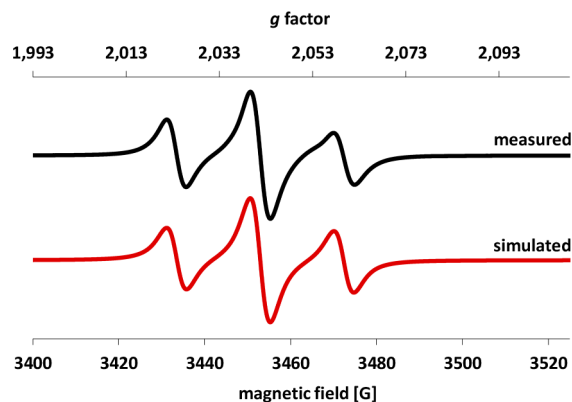


**Figure 2.** X-band EPR spectrum of [Fe(PCP<sup>Et</sup>-iPr)(CO)<sub>2</sub>] (4) in toluene at 293 K at a microwave frequency of 9.86 GHz. The red line represents a simulation with parameters *g*<sub>iso</sub> = 2.038 and *A* (<sup>31</sup>P) = 19.5 G.

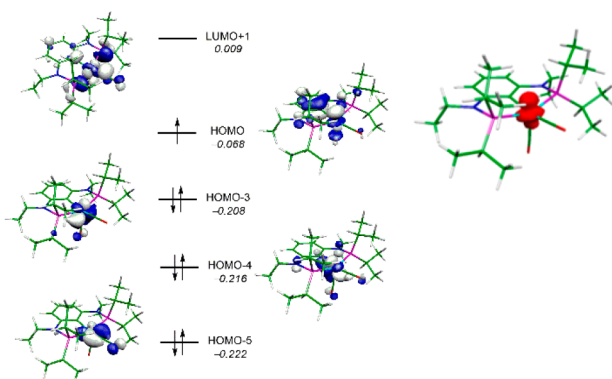


**Figure 3.** Frontier orbitals (*d*-splitting) and spin density for  $[\text{Fe}(\text{PCP}^{\text{Et}}\text{-iPr})(\text{CO})_2]$  (**4**).

coordinating atoms. The other three metal *d* orbitals, *xy*, *xz*, and *yz* are involved in filled molecular orbitals, HOMO-5, HOMO-4, and HOMO-3, respectively. Accordingly, the spin density of the molecule is located on the metal atom.

The solid-state structure of **4** was determined by X-ray diffraction. A view of the molecular structure is depicted in **Figure 4** with selected bond distances and angles reported in

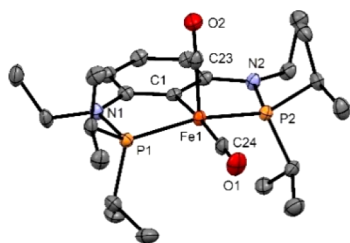
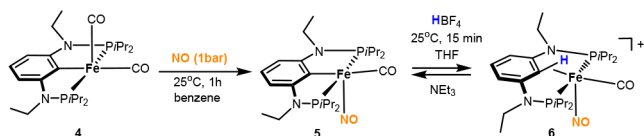


**Figure 4.** Structural view of  $[\text{Fe}(\text{PCP}^{\text{Et}}\text{-iPr})(\text{CO})_2]$  (**4**) showing 50% thermal ellipsoids (H atoms omitted for clarity). Selected bond lengths (Å) and bond angles (deg): Fe1–C1 2.015(3), Fe1–P1 2.1791(8), Fe1–P2 2.1868(8), Fe1–C24 1.772(3), Fe1–C23 1.774(3), P1–Fe1–P2 153.25(3), C24–Fe1–C23 97.5(1), C24–Fe1–C1 172.4(1).

the caption. The complex adopts square pyramidal geometry. The  $C_{\text{ipso}}\text{--Fe1}$  bond distance is 2.015(3) Å. The P–Fe–P, C<sub>CO</sub>–Fe–C<sub>CO</sub>, and C1–Fe1–C<sub>CO</sub> angles are 153.25(3), 97.5(1), and 172.4(1)°, respectively.

We then began to investigate the reactivity of complex **4**. Exposure of a benzene solution of **4** to NO (1 bar) at room temperature affords the diamagnetic complex  $[\text{Fe}(\text{PCP}^{\text{NEt}}\text{-iPr})(\text{CO})(\text{NO})]$  (**5**) in 71% isolated yield (**Scheme 3**). According to our knowledge, this is the first iron PCP nitrosyl complex. This reaction could be viewed as a formal one electron reduction of the metal center by the NO radical from Fe(I) to Fe(0), if NO is counted as NO<sup>+</sup>, or as an oxidation to Fe(II) with a negative ligand (NO<sup>-</sup>). This complex was again fully characterized by standard methods including NMR

### Scheme 3. Addition of NO to **4** and Reversible Protonation of **5**



spectroscopy, IR spectroscopy, and HR-MS analysis. The  $^{13}\text{C}\{^1\text{H}\}$  NMR spectrum gives rise to low-field triplet resonances at 228.3 ppm (t,  $J = 29.0$  Hz) assignable to the carbonyl carbon atom and a triplet resonance at 137.5 ppm ( $J_{\text{PC}} = 14.4$  Hz) assigned to the *ipso* carbon of the benzene moiety. In the IR spectrum two strong absorption bands assignable to the CO and NO stretching frequencies, respectively, are observed at 1890 and 1663  $\text{cm}^{-1}$  (cf. a related cationic complex  $[\text{Fe}(\text{PNP}^{\text{O}}\text{-iPr})(\text{CO})(\text{NO})]^+$  exhibits the respective stretching frequencies at 1948 and 1732  $\text{cm}^{-1}$ ).<sup>13</sup>

The oxidation state of Fe in complex **5** is not straightforward because the two electrons of the Fe–NO bond seem to be almost equally distributed among the metal and the ligand. However, the frontier orbitals (*d* splitting) obtained indicate a  $d^6$  species (see ESI) and the charge of the metal ( $C_{\text{Fe}} = -0.10$ ) is about half the value calculated for complex **4** ( $C_{\text{Fe}} = -0.19$ ) where the metal is unquestionably Fe(I). Those results suggest a metal oxidation state closer to Fe(II) than to Fe(0), in complex **5**. Interestingly, the Fe–N bond is very strong with a Wiberg index (WI) of 1.17.

Protonation of  $[\text{Fe}(\text{PCP}^{\text{NEt}}\text{-iPr})(\text{CO})(\text{NO})]$  (**5**) with  $\text{HBF}_4\cdot\text{Et}_2\text{O}$  leads to the formation of the cationic Fe(0) complex  $[\text{Fe}(\kappa^3\text{P,CH,P-P}(\text{CH})\text{P}^{\text{NEt}}\text{-iPr})(\text{CO})(\text{NO})]\text{BF}_4$  (**6**) in 95% isolated yield (**Scheme 3**). This complex features an agostic arene C–H bond. There was no evidence for the formation of the Fe(II) hydride complex  $[\text{Fe}(\text{PCP}^{\text{NMe}}\text{-iPr})(\text{CO})(\text{NO})(\text{H})]^+$ . DFT calculations reveal that such a hydride complex is thermodynamically less favorable by 10 kcal/mol. The agostic proton is comparatively acidic and thus readily deprotonated even with weak bases, such as  $\text{NEt}_3$ , thereby reforming the starting material **5**. Accordingly, this process is fully reversible (**Scheme 3**).

Complex **6** was again characterized by  $^1\text{H}$ ,  $^{13}\text{C}\{^1\text{H}\}$ , and  $^{31}\text{P}\{^1\text{H}\}$  NMR spectroscopy, IR, HR-MS, and X-ray crystallography. A characteristic feature of the  $^1\text{H}$  NMR spectrum is the high-field shift of the proton attached to the *ipso*-carbon giving rise to a triplet at 2.90 ppm ( $^4J_{\text{HP}} = 6.1$  Hz). In the  $^{13}\text{C}\{^1\text{H}\}$  NMR spectrum the *ipso*-carbon atom shows a signal at 66.5 ppm, and the CO ligand gives rise to a low-field resonance as triplet centered at 216.6 ppm ( $J_{\text{CP}} = 61.0$  Hz). The relatively low  $^1J_{\text{HC}}$  coupling constant of 125.6 Hz, as compared to 160.8 and 165.2 Hz for the other two aromatic C–H bonds, is also a typical feature of a strong C–H metal bond.<sup>4,14–22</sup> Complex **6** exhibits two bands at 1932 and 1720  $\text{cm}^{-1}$  in the IR spectrum assignable to the CO and NO stretching frequencies, respectively (cf. 1890 and 1663  $\text{cm}^{-1}$  in complex **4** which is more electron rich).

Contrarily to what was found for complex **5**, the frontier orbitals obtained for complex **6** (see Supporting Information and **Figure 5**) indicate a  $d^8$  complex and, thus, suggest an Fe(0) species. This conclusion is reinforced by the calculated

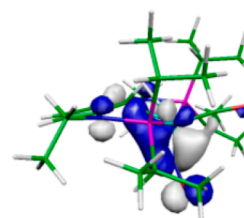


**Figure 5.** HOMO-2 of complex **6** showing  $\pi$ -backdonation from metal *d* to the C–H  $\sigma^*$  orbital.

charges. The NO ligand has a charge of  $C_{NO} = -0.06$ , being clearly electron poorer than in **5** ( $C_{NO} = -0.17$ ), while the metal is rather rich, in terms of electronic density, considering the cationic nature of the molecule ( $C_{Fe} = -0.06$ ).

The agostic Fe–(C–H) interaction is also reflected in the complex HOMO–2 that represents the characteristic  $\pi$ -backdonation from metal  $d$  to the C–H  $\sigma^*$  orbital (Figure 6). The weakening of the C–H bond due to the agostic

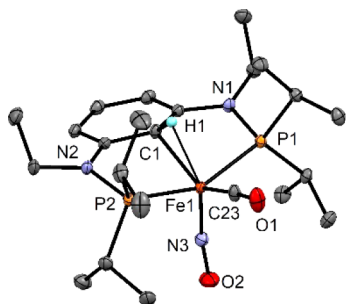


**Figure 6.** Structural view of  $[\text{Fe}(\kappa^3\text{P},\text{CH},\text{P}-\text{P}(\text{CH})\text{P}^{\text{NEt}}\text{-iPr})(\text{CO})(\text{NO})]\text{BF}_4$  (**6**) showing 50% thermal ellipsoids (most H atoms and  $\text{BF}_4^-$  counterion omitted for clarity). Selected bond lengths (Å) and bond angles (deg): Fe1–C1 2.158(1), Fe1–N3 1.672(1), Fe1–C23 1.761(1), Fe1–P2 2.2596(4), Fe1–P1 2.2690(4), Fe1–H1 1.94(2), C1–H1 1.0(2), N3–Fe1–C23 113.17(5), C23–Fe1–C1 136.24(5), P2–Fe1–P1 154.74(2).

interaction is evident from the longer bond distance ( $d_{\text{C–H}} = 1.11$  Å) and weaker WI of 0.80 when compared to the other  $\text{C}_{\text{aryl}}\text{–H}$  bonds ( $d = 1.08$  Å, WI = 0.91).

An ORTEP plot of complex **6** is presented in Figure 6. This compound exhibits essentially a trigonal bipyramidal geometry with the CO and NO ligands and the agostic C–H bond in the equatorial plane and the phosphine donors in the axial positions. The bond distance of the *ipso*-carbon and the Fe atom is rather long (2.258(1) Å) when compared to simple Fe–C  $\sigma$ -bonds. For example, in the Fe(II) and Fe(I) PCP complexes  $[\text{Fe}(\text{PCP}^{\text{NEt}}\text{-iPr})(\text{CO})_2\text{Cl}]$  (**2**) and  $[\text{Fe}(\text{PCP}^{\text{NEt}}\text{-iPr})(\text{CO})_2]$  (**4**) the Fe– $\text{C}_{\text{ipso}}$  bond distances are significantly shorter, being 2.002(2) and 2.015(3) Å, respectively. The H(1) atom could be located in difference Fourier maps and was refined freely. This hydrogen atom clearly interacts with the Fe center as evident from a Fe–H bond length of 1.94(2) Å and is also supported by the  $^1\text{H}$  NMR spectrum of **6** as discussed above. Moreover, this hydrogen is severely bent away from the benzene plane by ca.  $29.2^\circ$  (cf. in similar Ru, Rh, and Pd pincer complexes this angle is about  $14\text{--}30^\circ$ ,<sup>14–22</sup> while in Cr, Mo,<sup>4</sup> and Co<sup>14</sup> it is  $32$ ,  $28$ , and  $35^\circ$ , respectively). The C1–H1 bond distance is 1.0(2) Å, which is comparable to hydrocarbons such as 1.08 Å in benzene.

## CONCLUSION

We described here the preparation of the Fe(II) PCP complex  $[\text{Fe}(\text{PCP}^{\text{NEt}}\text{-iPr})(\text{CO})_2\text{Cl}]$  (**2**). Under solvothermal conditions, treatment of  $\text{Fe}_2(\text{CO})_9$  with 2-chloro- $N^1,N^3$ -bis-(diisopropylphosphanyl)- $N^1,N^3$ -diethylbenzene-1,3-diamine ( $\text{P}(\text{C–Cl})\text{P}^{\text{NEt}}\text{-iPr}$ ) (**1**) in  $\text{CH}_3\text{CN}$  in a sealed microwave glass vial for 18 h at  $110^\circ\text{C}$  afforded complex **2** in 47% isolated yield. In an endeavor to obtain the hydride Fe(II) complex  $[\text{Fe}(\text{PCP}^{\text{NEt}}\text{-iPr})(\text{CO})_2\text{H}]$  (**3**), complex **2** was treated with  $\text{Li}[\text{HBEt}_3]$  in THF. However, instead of ligand substitution, this complex was reduced to the low-spin  $d^7$  Fe(I) complex

$[\text{Fe}(\text{PCP}^{\text{NEt}}\text{-iPr})(\text{CO})_2]$  (**4**). Exposure of a benzene solution of complex **4** to NO gas (1 bar) at room temperature resulted in the substitution of a CO ligand with a concomitant one-electron reduction of the metal center to afford the diamagnetic complex  $[\text{Fe}(\text{PCP}^{\text{NEt}}\text{-iPr})(\text{CO})(\text{NO})]$  (**5**). DFT calculations suggest a metal oxidation state closer to Fe(II) than to Fe(0). This is the first iron PCP nitrosyl complex. Protonation of **5** with  $\text{HBF}_4\cdot\text{Et}_2\text{O}$  leads to the formation of the cationic Fe(0) complex  $[\text{Fe}(\kappa^3\text{P},\text{CH},\text{P}-\text{P}(\text{CH})\text{P}^{\text{NEt}}\text{-iPr})(\text{CO})(\text{NO})]\text{BF}_4$  (**6**), which features an  $\eta^2\text{-C}_{\text{aryl}}\text{–H}$  agostic bond. The agostic proton is comparatively acidic and thus readily deprotonated even with weak bases, such as  $\text{NEt}_3$ , thereby reforming the starting material **5**. Accordingly, this process is fully reversible.

## EXPERIMENTAL SECTION

**General Information.** All reactions were performed under an inert atmosphere of argon by using Schlenk techniques or in a MBraun inert-gas glovebox. The solvents were purified according to standard procedures.<sup>23</sup> The deuterated solvents were purchased from Aldrich and dried over 3 Å molecular sieves. The synthesis of 2-chloro- $N^1,N^3$ -bis-(diisopropylphosphanyl)- $N^1,N^3$ -diethylbenzene-1,3-diamine ( $\text{P}(\text{C–Cl})\text{P}^{\text{NEt}}\text{-iPr}$ ) (**1**) is described in the Supporting Information. All starting materials are known compounds and were used as obtained from commercial resources.  $^1\text{H}$  and  $^{13}\text{C}\{^1\text{H}\}$  and  $^{31}\text{P}\{^1\text{H}\}$  NMR spectra were recorded on Bruker AVANCE-250, AVANCE-400, and AVANCE-600 spectrometers.  $^1\text{H}$  and  $^{13}\text{C}\{^1\text{H}\}$  NMR spectra were referenced internally to residual protio-solvent and solvent resonances, respectively, and are reported relative to tetramethylsilane ( $\delta = 0$  ppm).  $^{31}\text{P}\{^1\text{H}\}$  NMR spectra were referenced externally to  $\text{H}_3\text{PO}_4$  (85%) ( $\delta = 0$  ppm).

High resolution-accurate mass data mass spectra were recorded on a hybrid Maxis Qq-aoTOF mass spectrometer (Bruker Daltonics, Bremen, Germany) fitted with an ESI-source. Measured accurate mass data of the  $[\text{M}]^+$  ions for confirming calculated elemental compositions were typically within  $\pm 5$  ppm accuracy. The mass calibration was done with a commercial mixture of perfluorinated trialkyl-triazines (ES Tuning Mix, Agilent Technologies, Santa Clara, CA, USA).

CW-EPR spectroscopic measurements were performed on an X-band Bruker Elexsys-II E500 EPR spectrometer (Bruker Biospin GmbH, Rheinstetten, Germany) in solution at 293 K. A high sensitivity cavity (SHQE1119) was used for measurements setting the microwave frequency to 9.86 GHz, the modulation frequency to 100 kHz, the center field to 6000 G, the sweep width to 12000 G, the sweep time to 30.0 s, the modulation amplitude to 6 G, the microwave power to 15.9 mW, the conversion time to 7.33 ms, and the resolution to 4096 points. The spectra were analyzed using the Bruker Xepr software.

**Synthesis.**  $[\text{Fe}(\text{PCP}^{\text{NEt}}\text{-iPr})(\text{CO})_2\text{Cl}]$  (**2**). A suspension of  $[\text{Fe}_2(\text{CO})_9]$  (151 mg, 0.42 mmol) and 2 equivs of **1** (200 mg, 0.84 mmol) in  $\text{CH}_3\text{CN}$  (2 mL) were placed in a 20 mL sealed glass tube and stirred for 18 h at  $110^\circ\text{C}$ . The reaction mixture was allowed to cool to room temperature without stirring. Insoluble materials were removed by filtration over a syringe filter (polytetrafluoroethylene 0.2  $\mu\text{m}$ ), and the solvent was removed under vacuum. The product was obtained as yellow powder and washed three times with pentane. Yield: 118 mg (47%). Anal. Calcd for  $\text{C}_{24}\text{H}_{41}\text{ClFeN}_2\text{O}_2\text{P}_2$  (542.85): C, 53.10; H, 7.61; N, 5.16. Found: C, 53.35; H, 7.59; N, 5.20.  $^1\text{H}$  NMR ( $\delta$ , 600 MHz,  $\text{C}_6\text{D}_6$ ,  $20^\circ\text{C}$ ): 7.20 (t,  $J = 8.1$  Hz, 1H,  $\text{C}_{\text{ar}}\text{H}$ ), 6.27 (d,  $J = 8.0$  Hz, 2H,  $\text{C}_{\text{ar}}\text{H}$ ), 3.10 (m, 4H, N– $\text{CH}_2$ ), 2.92 (m, 2H, P–CH), 2.34 (m, 2H, P–CH), 1.46 (q,  $J = 7.7$  Hz, 6H, CH– $\text{CH}_3$ ), 1.25 (q,  $J = 7.1$  Hz, 6H, CH– $\text{CH}_3$ ), 1.20 (q,  $J = 7.5$  Hz, 6H, CH– $\text{CH}_3$ ), 1.11 (q,  $J = 7.1$  Hz, 6H, CH– $\text{CH}_3$ ), 1.05 (t, 6H,  $J = 6.9$  Hz,  $\text{CH}_2\text{–CH}_3$ ).  $^{13}\text{C}\{^1\text{H}\}$  NMR ( $\delta$ , 600 MHz,  $\text{C}_6\text{D}_6$ ,  $20^\circ\text{C}$ ): 215.6 (t,  $J = 27.4$  Hz, CO), 212.7 (t,  $J = 11.6$  Hz, CO), 156.8 (t,  $J = 13.7$  Hz, C–N), 137.5 (t,  $J = 14.4$  Hz, C–Fe), 126.6 (s,  $\text{C}_{\text{ar}}\text{H}$ ), 103.0 (t,  $J = 5.4$  Hz,  $\text{C}_{\text{ar}}\text{H}$ ), 41.0 (s,  $\text{CH}_2$ ), 30.7 (t,  $J = 11.6$  Hz, P–CH), 29.0 (t,  $J = 11.0$  Hz, P–CH), 22.1 (s, CH–

CH<sub>3</sub>), 19.5 (s, CH-CH<sub>3</sub>), 19.5 (s, CH-CH<sub>3</sub>), 18.9 (t, *J* = 3.4 Hz, CH-CH<sub>3</sub>), 14.2 (s, CH<sub>2</sub>-CH<sub>3</sub>). <sup>31</sup>P{<sup>1</sup>H} NMR (δ, 250 MHz, C<sub>6</sub>D<sub>6</sub>, 20 °C): 151.5. HR-MS (ESI<sup>+</sup>, CH<sub>3</sub>CN/MeOH+1%H<sub>2</sub>O): *m/z* calcd for C<sub>24</sub>H<sub>41</sub>FeN<sub>2</sub>O<sub>2</sub>P<sub>2</sub> [M - Cl]<sup>+</sup> 507.1993, found 507.1990. IR (ATR, cm<sup>-1</sup>): 2002 (ν<sub>CO</sub>), 1934 (ν<sub>CO</sub>).

[Fe(PCP<sup>NEt</sup>-iPr)(CO)]<sub>2</sub> (4). A solution of 2 (50 mg, 0.092 mmol) in THF (3 mL) was reacted Li[HB(Et)<sub>3</sub>] (0.06 mL, 1.7 M solution in THF, 0.10 mmol) at room temperature and stirred for 1 h. The color of the solution instantly changed from orange to dark violet. All volatiles were removed under vacuum and an oily residue was obtained. The product was redissolved in pentane and filtered over a syringe filter (polytetrafluoroethylene 0.2 μm). Crystals could be obtained by cooling the pentane solution to -30 °C for 24 h. Yield: 43 mg (93%). Anal. Calcd for C<sub>24</sub>H<sub>41</sub>FeN<sub>2</sub>O<sub>2</sub>P<sub>2</sub> (507.40): C, 56.81; H, 8.15; N, 5.52. Found: C, 56.95; H, 8.39; N, 5.45. HR-MS (ESI<sup>+</sup>, CH<sub>3</sub>CN/MeOH + 1%H<sub>2</sub>O) *m/z* calcd for C<sub>23</sub>H<sub>41</sub>FeN<sub>2</sub>O<sub>2</sub>P<sub>2</sub> [M - CO]<sup>+</sup> 479.2044, found 479.2038. μ<sub>eff</sub> = 1.8(1) μ<sub>B</sub> (benzene, Evans method). IR (ATR, cm<sup>-1</sup>): 1937 (ν<sub>CO</sub>), 1866 (ν<sub>CO</sub>).

[Fe(PCP<sup>NEt</sup>-iPr)(CO)(NO)] (5). A solution of 4 (80 mg, 0.16 mmol) in benzene (2 mL) was stirred for 1 h under an NO gas atmosphere (1 bar) whereupon the solution turned from dark violet to red. Insoluble materials were removed by filtration through a syringe filter (polytetrafluoroethylene 0.2 μm). After removal of the solvent under vacuum, the product was obtained as a red solid. Yield: 57 mg (71%). Anal. Calcd for C<sub>23</sub>H<sub>41</sub>FeN<sub>3</sub>O<sub>2</sub>P<sub>2</sub> (509.39): C, 54.23; H, 8.11; N, 8.25. Found: C, 54.37; H, 8.09; N, 8.10. <sup>1</sup>H NMR (δ, 600 MHz, C<sub>6</sub>D<sub>6</sub>, 20 °C): 7.19 (t, *J* = 7.8 Hz, 1H, C<sub>ar</sub>H), 6.21 (d, *J* = 7.8 Hz, 2H, C<sub>ar</sub>H), 3.15 (m, 2H, N-CH<sub>2</sub>), 3.03 (m, 2H, N-CH<sub>2</sub>), 2.39 (m, 2H, P-CH), 2.30 (h, *J* = 7.1 Hz, 2H, P-CH), 1.33 (m, 6H, CH-CH<sub>3</sub>), 1.08 (dt, *J* = 7.1 Hz, *J* = 14.2 Hz, 12H, CH-CH<sub>3</sub>, CH<sub>2</sub>CH<sub>3</sub>), 0.99 (q, *J* = 7.4 Hz, 6H, CH-CH<sub>3</sub>), 0.90 (q, *J* = 7.0 Hz, 6H, CH-CH<sub>3</sub>). <sup>13</sup>C{<sup>1</sup>H} NMR (δ, 600 MHz, C<sub>6</sub>D<sub>6</sub>, 20 °C): 228.3 (t, *J* = 29.0 Hz, CO), 157.9 (t, *J* = 15.4 Hz, C-N), 137.4 (t, *J* = 24.1 Hz, C-Fe), 126.9 (s, C<sub>ar</sub>H), 101.5 (t, *J* = 6.2 Hz, C<sub>ar</sub>H), 40.3 (s, CH<sub>2</sub>), 31.8 (t, *J* = 11.0 Hz, P-CH), 28.1 (t, *J* = 13.6 Hz, P-CH), 18.2 (s, CH-CH<sub>3</sub>), 17.9 (s, CH-CH<sub>3</sub>), 17.2 (s, CH-CH<sub>3</sub>), 17.1 (t, *J* = 4.1 Hz, CH-CH<sub>3</sub>), 14.2 (s, CH<sub>2</sub>-CH<sub>3</sub>). <sup>31</sup>P{<sup>1</sup>H} NMR (δ, 250 MHz, C<sub>6</sub>D<sub>6</sub>, 20 °C): 171.6. HR-MS (ESI<sup>+</sup>, CH<sub>3</sub>CN/MeOH + 1%H<sub>2</sub>O): *m/z* calcd for C<sub>22</sub>H<sub>41</sub>FeN<sub>3</sub>O<sub>2</sub>P<sub>2</sub> 481.2074 [M - CO]<sup>+</sup>, found 481.2075. IR (ATR, cm<sup>-1</sup>): 1890 (ν<sub>CO</sub>), 1663 (ν<sub>NO</sub>).

[Fe(*k*<sup>3</sup>P,CH,P-P(CH)<sup>NEt</sup>-iPr)(CO)(NO)]BF<sub>4</sub> (6). A solution of 5 (57 mg, 0.11 mmol) in THF (2 mL) was treated with HBF<sub>4</sub>·Et<sub>2</sub>O (24 mg, 0.15 mmol) and the reaction mixture was stirred for 15 min at room temperature. All volatiles were then removed under vacuum, and a red solid was obtained which was washed with ether (2 × 5 mL) and dried under vacuum. Yield: 65 mg (95%). Anal. Calcd for C<sub>23</sub>H<sub>42</sub>BF<sub>4</sub>FeN<sub>3</sub>O<sub>2</sub>P<sub>2</sub> (597.20): C, 46.26; H, 7.09; N, 7.04. Found: C, 46.39; H, 7.12; N, 7.13. <sup>1</sup>H NMR (δ, 600 MHz, CD<sub>3</sub>CN, 20 °C): 7.66 (tt, *J* = 8.2 Hz, *J* = 1.5 Hz, 1H, C<sub>ar</sub>H), 6.56 (d, *J* = 8.3 Hz, 2H, C<sub>ar</sub>H), 3.76 (m, 2H, N-CH<sub>2</sub>), 3.57 (m, 2H, N-CH<sub>2</sub>), 2.98 (m, 2H, P-CH), 2.90 (t, *J* = 6.1 Hz, 1H, CH-Fe), 2.82 (m, 2H, P-CH), 1.38 (dd, *J* = 18.0 Hz, *J* = 7.1 Hz, 6H, CH-CH<sub>3</sub>), 1.33 (dd, *J* = 16.1 Hz, *J* = 7.1 Hz, 6H, CH-CH<sub>3</sub>), 1.20 (t, *J* = 7.1 Hz, 6H, CH<sub>2</sub>-CH<sub>3</sub>), 1.16 (dd, *J* = 20.9 Hz, *J* = 7.0 Hz, 6H, CH-CH<sub>3</sub>), 1.03 (dd, *J* = 17.0 Hz, *J* = 7.0 Hz, 6H, CH-CH<sub>3</sub>). <sup>13</sup>C{<sup>1</sup>H} NMR (δ, 600 MHz, CD<sub>3</sub>CN, 20 °C): 216.6 (t, *J* = 61.0 Hz, CO), 167.5 (t, *J* = 10.2 Hz, C-N), 142.7 (s, C<sub>ar</sub>H), 107.4 (t, *J* = 4.2 Hz, C<sub>ar</sub>H), 66.5 (t, *J* = 3.4 Hz, CH-Fe), 41.7 (s, CH<sub>2</sub>), 30.9 (t, *J* = 14.0 Hz, P-CH), 30.0 (t, *J* = 11.5 Hz, P-CH), 18.2 (s, CH-CH<sub>3</sub>), 17.7 (s, CH-CH<sub>3</sub>), 16.9 (s, CH-CH<sub>3</sub>), 15.2 (t, *J* = 4.0 Hz, CH-CH<sub>3</sub>), 13.2 (s, CH<sub>2</sub>-CH<sub>3</sub>). <sup>31</sup>P{<sup>1</sup>H} NMR (δ, 250 MHz, CD<sub>3</sub>CN, 20 °C): 142.2. HR-MS (ESI<sup>+</sup>, CH<sub>3</sub>CN/MeOH + 1%H<sub>2</sub>O) *m/z*: calcd for C<sub>22</sub>H<sub>41</sub>FeN<sub>3</sub>O<sub>2</sub>P<sub>2</sub> 481.2074 [M - H - CO]<sup>+</sup>, found 481.2068. IR (ATR, cm<sup>-1</sup>): 1932 (ν<sub>CO</sub>), 1720 (ν<sub>NO</sub>).

**X-ray Structure Determination.** X-ray diffraction data of 2, 4, and 6 were collected at *T* = 100 K in a dry stream of nitrogen on a Bruker Kappa APEX II diffractometer system using graphite-monochromatized Mo Kα radiation (λ = 0.71073 Å) and fine sliced φ- and ω-scans. Data were reduced to intensity values with SAINT, and an absorption correction was applied with the multiscan approach implemented in SADABS.<sup>24</sup> The structure was solved by the dual-

space approach implemented in SHELXT<sup>25</sup> and refined against F<sup>2</sup> with SHELXL.<sup>26</sup> Non-hydrogen atoms were refined anisotropically. The H atoms connected to C atoms were placed in calculated positions and thereafter refined as riding on the parent atoms. The agostic H was located from difference Fourier maps and refined freely. The Cl ligands and the CO ligands in the *trans*-position to Cl in 2 were refined as occupationally disordered (occupancies constrained to reflect the nominal composition; minor positions realized to 39.4(10)% and 37.9(10)% for both crystallographically independent complexes, respectively). A part of the PCP ligand was refined as positionally disordered, with the occupancies constrained to those of the Cl/CO disorder. The Fe atom in 4 was refined as disordered about two positions (sum of occupancies constrained to 1; ADPs constrained to be identical; refined occupancy of the minor position 2.79(8)%). A peak in the difference electron map located ca. 2.4 Å from the minor Fe position suggests a cocrystallization with the chloride precursor. Although placing a Cl atom in this position led to convergence, it did not improve the reliability factors and was omitted in the final model. In 6, the Fe atom was likewise modeled as disordered about two positions. Owing to the absence of secondary species in the NMR spectra, we suppose a different orientation of the molecule. Since the minor position is only realized in 1.18% of the molecules, no significant peaks are observed in the difference Fourier maps and no definite statement can be made. Molecular graphics were generated with the program MERCURY.<sup>27</sup>

**Computational Details.** The computational results presented have been achieved in part using the Vienna Scientific Cluster (VSC). Calculations were performed using the GAUSSIAN 09 software package<sup>28</sup> and the B3LYP functional, without symmetry constraints. That functional includes a mixture of Hartree-Fock<sup>29</sup> exchange with DFT<sup>30</sup> exchange-correlation, given by Becke's three parameter functional<sup>31</sup> with the Lee, Yang, and Parr correlation functional, which includes both local and nonlocal terms.<sup>32,33</sup> The basis set used consisted of the Stuttgart/Dresden ECP (SDD) basis set<sup>34</sup> to describe the electrons of Fe and a standard 6-31G(d,p) basis set<sup>35</sup> for all other atoms. The frontier orbitals of complex 4 result from a single point restricted open shell calculation. A Natural Population Analysis (NPA)<sup>36</sup> and the resulting Wiberg indices<sup>37</sup> were used to study the electronic structure and bonding of the optimized species. The NPA analysis was performed with the NBO 5.0 program,<sup>38</sup> and the three-dimensional representations of the orbitals were obtained with Molekel.<sup>39</sup>

## ■ ASSOCIATED CONTENT

### 📄 Supporting Information

The Supporting Information is available free of charge on the ACS Publications website at DOI: 10.1021/acs.inorgchem.8b01018.

Complete crystallographic data, <sup>1</sup>H, <sup>13</sup>C{<sup>1</sup>H}, and <sup>31</sup>P{<sup>1</sup>H} NMR spectra of all complexes (PDF)

### Accession Codes

CCDC 1836427–1836429 contain the supplementary crystallographic data for this paper. These data can be obtained free of charge via [www.ccdc.cam.ac.uk/data\\_request/cif](http://www.ccdc.cam.ac.uk/data_request/cif), or by emailing [data\\_request@ccdc.cam.ac.uk](mailto:data_request@ccdc.cam.ac.uk), or by contacting The Cambridge Crystallographic Data Centre, 12 Union Road, Cambridge CB2 1EZ, UK; fax: +44 1223 336033.

## ■ AUTHOR INFORMATION

### Corresponding Author

\*K.K.: E-mail, [karl.kirchner@tuwien.ac.at](mailto:karl.kirchner@tuwien.ac.at); tel, (+43) 1 58801 163611; fax, (+43) 1 58801 16399.

### ORCID

Luis F. Veiros: 0000-0001-5841-3519

Marc Pignitter: 0000-0002-5793-8572

Veronika Somoza: 0000-0003-2456-9245

Karl Kirchner: 0000-0003-0872-6159

## Notes

The authors declare no competing financial interest.

## ACKNOWLEDGMENTS

Financial support by the Austrian Science Fund (FWF) is gratefully acknowledged (Project No. P29584-N28). LFV acknowledges Fundação para a Ciência e Tecnologia, UID/QUI/00100/2013.

## REFERENCES

(1) Coining of the name “pincer”: van Koten. Tuning the reactivity of metals held in a rigid ligand environment *G. Pure Appl. Chem.* **1989**, *61*, 1681–1694.

(2) For reviews on pincer complexes, see: (a) Gossage, R. A.; van de Kuil, L. A.; van Koten, G. Diaminoarylnickel(II) “pincer” complexes: mechanistic consideration in the Kharasch addition reaction, controlled polymerization, and dendrimeric transition metal catalysis. *Acc. Chem. Res.* **1998**, *31*, 423–431. (b) Albrecht, M.; van Koten, G. Platinum group organometallics based on “Pincer” complexes: sensors, switches, and catalysts in memory of Prof. Dr. Luigi M. Venanzi and his pioneering work in organometallic chemistry, particularly in PCP pincer chemistry. *Angew. Chem., Int. Ed.* **2001**, *40*, 3750–3781. (c) van der Boom, M. E.; Milstein, D. Cyclo-metalated phosphine-based pincer complexes: mechanistic insight in catalysis, coordination, and bond activation. *Chem. Rev.* **2003**, *103*, 1759–1792. (d) Singleton, J. T. The uses of pincer complexes in organic synthesis. *Tetrahedron* **2003**, *59*, 1837–1857. (e) Liang, L. C. Metal complexes of chelating diarylamido phosphine ligands. *Coord. Chem. Rev.* **2006**, *250*, 1152–1177. (f) *The Chemistry of Pincer Compounds*; Morales-Morales, D.; Jensen, C. M.; Eds.; Elsevier: Amsterdam, 2007. (g) Nishiyama, H. Synthesis and use of bisoxazolanyl-phenyl pincers. *Chem. Soc. Rev.* **2007**, *36*, 1133–1141. (h) Benito-Garagorri, D.; Kirchner, K. Modularly Designed Transition Metal PNP and PCP Pincer Complexes Based on Aminophosphines: Synthesis and Catalytic Applications. *Acc. Chem. Res.* **2008**, *41*, 201–213. (i) Choi, J.; MacArthur, A. H. R.; Brookhart, M.; Goldman, A. S. Dehydrogenation and Related Reactions Catalyzed by Iridium Pincer Complexes. *Chem. Rev.* **2011**, *111*, 1761–1779. (j) Selander, N.; Szabo, K. J. Catalysis by Palladium Pincer Complexes. *Chem. Rev.* **2011**, *111*, 2048–2076. (k) Bhattacharya, P.; Guan, H. Synthesis and Catalytic Applications of Iron Pincer Complexes. *Comments Inorg. Chem.* **2011**, *32*, 88–112. (l) Schneider, S.; Meiners, J.; Askevold, B. Cooperative Aliphatic PNP Amido Pincer Ligands - Versatile Building Blocks for Coordination Chemistry and Catalysis. *Eur. J. Inorg. Chem.* **2012**, *2012*, 412–429. (m) van Koten, G.; Milstein, D., Eds.; *Organometallic Pincer Chemistry*; Springer: Berlin, 2013; Top. Organomet. Chem. Vol. 40. (n) Szabo, K. J.; Wendt, O. F. *Pincer and Pincer-Type Complexes: Applications in Organic Synthesis and Catalysis*; Wiley-VCH: Germany, 2014. (o) Asay, M.; Morales-Morales, D. Non-symmetric pincer ligands: complexes and applications in catalysis. *Dalton Trans.* **2015**, *44*, 17432–17447. (p) Murugesan, S.; Kirchner, K. Non-precious metal complexes with an anionic PCP pincer architecture. *Dalton Trans.* **2016**, *45*, 416–439.

(3) For recent reviews on C-H activation and functionalization, see: (a) Jia, C.; Kitamura, T.; Fujiwara, Y. Catalytic Functionalization of Arenes and Alkanes via C–H Bond Activation. *Acc. Chem. Res.* **2001**, *34*, 633–639. (b) Ritleng, V.; Sirlin, C.; Pfeffer, M. Ru-, Rh-, and Pd-Catalyzed C–C Bond Formation Involving C–H Activation and Addition on Unsaturated Substrates: Reactions and Mechanistic Aspects. *Chem. Rev.* **2002**, *102*, 1731–1770. (c) Colby, D. A.; Bergman, R. G.; Ellman, J. A. Rhodium-Catalyzed C–C Bond Formation via Heteroatom-Directed C–H Bond Activation. *Chem. Rev.* **2010**, *110*, 624–655. (d) Arockiam, P. B.; Bruneau, C.; Dixneuf, P. H. Ruthenium(II)-Catalyzed C–H Bond Activation and Functionalization. *Chem. Rev.* **2012**, *112*, 5879–5918. (e) Lewis, J.

C.; Bergman, R. G.; Ellman, J. A. Direct Functionalization of Nitrogen Heterocycles via Rh-Catalyzed C–H Bond Activation. *Acc. Chem. Res.* **2008**, *41*, 1013–1025. (f) Gaillard, S.; Cazin, C. S. J.; Nolan, S. P. N-Heterocyclic Carbene Gold(I) and Copper(I) Complexes in C–H Bond Activation. *Acc. Chem. Res.* **2012**, *45*, 778–787. (g) Li, B.; Dixneuf, P. H.  $sp^2$  C–H bond activation in water and catalytic cross-coupling reactions. *Chem. Soc. Chem. Soc. Rev.* **2013**, *42*, 5744–5767. (h) Wencel-Delord, J.; Dröge, T.; Liu, F.; Glorius, F. Towards mild metal-catalyzed C–H bond activation. *Chem. Soc. Rev.* **2011**, *40*, 4740–4761.

(4) de Aguiar, S. R. M. M.; Stöger, B.; Pittenauer, E.; Allmaier, G.; Veiros, L. F.; Kirchner, K. Arene C–H Bond Coordination versus C–H Bond Cleavage in Low-Valent Group 6 Carbonyl Pincer Complexes. *Organometallics* **2016**, *35*, 3032–3039.

(5) Bhattacharya, P.; Krause, J. A.; Guan, H. Iron Hydride Complexes Bearing Phosphinite-Based Pincer Ligands: Synthesis, Reactivity, and Catalytic Application in Hydrosilylation Reactions. *Organometallics* **2011**, *30*, 4720–4729.

(6) Bhattacharya, P.; Krause, J. A.; Guan, H. Mechanistic Studies of Ammonia Borane Dehydrogenation Catalyzed by Iron Pincer Complexes. *J. Am. Chem. Soc.* **2014**, *136*, 11153–11161.

(7) Bhattacharya, P.; Krause, J. A.; Guan, H. Activation of Dihydrogen and Silanes by Cationic Iron Bis(phosphinite) Pincer Complexes. *Organometallics* **2014**, *33*, 6113–6121.

(8) Jiang, S.; Quintero-Duque, S.; Roisnel, T.; Dorcet, V.; Grellier, M.; Sabo-Etienne, S.; Darcel, C.; Sortais, J.-B. Direct synthesis of dicarbonyl PCP-iron hydride complexes and catalytic dehydrogenative borylation of styrene. *Dalton Trans.* **2016**, *45*, 11101–11108.

(9) Dauth, A.; Gellrich, U.; Diskin-Posner, Y.; Ben-David, Y.; Milstein, D. The Ferraquinone–Ferrahydroquinone Couple: Combining Quinonic and Metal-Based Reactivity. *J. Am. Chem. Soc.* **2017**, *139*, 2799–2807.

(10) Thompson, C. V.; Arman, H. D.; Tonzetich, Z. J. A Pyrrole-Based Pincer Ligand Permits Access to Three Oxidation States of Iron in Organometallic Complexes. *Organometallics* **2017**, *36*, 1795–1802.

(11) (a) Kuriyama, S.; Arashiba, K.; Nakajima, K.; Matsuo, Y.; Tanaka, H.; Ishii, K.; Yoshizawa, K.; Nishibayashi, Y. Catalytic transformation of dinitrogen into ammonia and hydrazine by iron-dinitrogen complexes bearing pincer ligand. *Nat. Commun.* **2016**, *7*, 12181. (b) Kupper, C.; Schober, A.; Demeshko, S.; Bergner, M.; Meyer, F. An Exclusively Organometallic  $\{FeNO\}^7$  Complex with Tetracarbene Ligation and a Linear FeNO Unit. *Inorg. Chem.* **2015**, *54*, 3096–3098. (c) Ehrlich, N.; Kreye, M.; Baabe, D.; Schweyen, P.; Freytag, M.; Jones, P. G.; Walter, M. D. Synthesis and Electronic Ground-State Properties of Pyrrolyl-Based Iron Pincer Complexes: Revisited. *Inorg. Chem.* **2017**, *56*, 8415–8422. (d) Thompson, C. V.; Davis, I.; DeGayner, J. A.; Arman, H. D.; Tonzetich, Z. J. Iron Pincer Complexes Incorporating Bipyridine: A Strategy for Stabilization of Reactive Species. *Organometallics* **2017**, *36*, 4928–4935.

(12) Albright, T. A.; Burdett, J. K.; Whangbo, M.-H. *Orbital Interactions in Chemistry*; John Wiley & Sons: New York, 1985; p 312.

(13) Tondreau, A. M.; Boncella, J. M. The synthesis of PNP-supported low-spin nitro manganese(I) carbonyl complexes. *Polyhedron* **2016**, *116*, 96–104.

(14) Murugesan, S.; Stöger, B.; Pittenauer, E.; Allmaier, G.; Veiros, L. F.; Kirchner, K. A Cobalt(I) Pincer Complex with an  $\eta(2)$ -C(aryl)-H Agostic Bond: Facile C-H Bond Cleavage through Deprotonation, Radical Abstraction, and Oxidative Addition. *Angew. Chem., Int. Ed.* **2016**, *55*, 3045–3048.

(15) (a) Vigalok, A.; Uzan, O.; Shimon, L. J. W.; Ben-David, Y.; Martin, J. L.; Milstein, D. Formation of  $\eta^2$  C–H Agostic Rhodium Arene Complexes and Their Relevance to Electrophilic Bond Activation. *J. Am. Chem. Soc.* **1998**, *120*, 12539–12544. (b) Vigalok, A.; Rybtchinski, B.; Shimon, L. J. W.; Ben-David, Y.; Milstein, D. Metal-Stabilized Methylene Arenium and  $\sigma$ -Arenium Compounds: Synthesis, Structure, Reactivity, Charge Distribution, and Interconversion. *Organometallics* **1999**, *18*, 895–905. (c) Montag, M.; Schwartsburd, L.; Cohen, R.; Leitun, G.; Ben-David, Y.; Martin, J. M. L.; Milstein, D. The Unexpected Role of CO in C-H Oxidative

- Addition by a Cationic Rhodium(I) Complex. *Angew. Chem., Int. Ed.* **2007**, *46*, 1901–1904. (d) Frech, C. M.; Shimon, L. J. W.; Milstein, D. Unsaturated Rh(I) and Rh(III) Naphthyl-Based PCP Complexes. Major Steric Effect on Reactivity. *Organometallics* **2009**, *28*, 1900–1908. (e) Montag, M.; Efremenko, I.; Cohen, R.; Shimon, L. J. W.; Leitens, G.; Diskin-Posner, Y.; Ben-David, Y.; Salem, H.; Martin, J. M. L.; Milstein, D. Effect of CO on the Oxidative Addition of Arene C-H Bonds by Cationic Rhodium Complexes. *Chem. - Eur. J.* **2010**, *16*, 328–353.
- (16) Albeniz, A. C.; Schulte, G.; Crabtree, R. H. Facile reversible metalation in an agostic complex and hydrogenolysis of a metal aryl complex via a dihydrogen complex. *Organometallics* **1992**, *11*, 242–249.
- (17) (a) Dani, P.; Karlen, T.; Gossage, R. A.; Smeets, W. J. J.; Spek, A. L.; van Koten, G. Replacement of a Cyclometalated Terdentate Diamino Ligand by a Phosphorus Analogue. Isolation and Crystallographic Characterization of an Intermediate in Aryl C–H Bond Activation in Models of Dendrimer-Bound Organometallic Catalysts. *J. Am. Chem. Soc.* **1997**, *119*, 11317–11318. (b) Dani, P.; Toorneman, M. A. M.; van Klink, G. P. M.; van Koten, G. Complexes of Bis-orthocyclometalated Bisphosphinoaryl Ruthenium(II) Cations with Neutral Meta-bisphosphinoarene Ligands Containing an Agostic C–H...Ru Interaction. *Organometallics* **2000**, *19*, 5287–5296.
- (18) McLoughlin, M. A.; Flesher, R. J.; Kaska, W. C.; Mayer, H. A. Synthesis and Reactivity of  $[\text{IrH}_2(\text{tBu}_2\text{P})\text{CH}_2\text{CH}_2\text{CHCH}_2\text{CH}_2\text{P}(\text{tBu}_2)]$ , a Dynamic Iridium Polyhydride Complex. *Organometallics* **1994**, *13*, 3816–3822.
- (19) van der Boom, M. E.; Iron, M. A.; Atasoylu, O.; Shimon, L. J. W.; Rozenberg, H.; Ben-David, Y.; Konstantinovski, L.; Martin, J. M. L.; Milstein, D.  $\text{sp}^3$  C–H and  $\text{sp}^2$  C–H agostic ruthenium complexes: a combined experimental and theoretical study. *Inorg. Chim. Acta* **2004**, *357*, 1854–1864.
- (20) Gusev, D. G.; Madott, M.; Dolgushin, F. M.; Lyssenko, K. A.; Antipin, M. Yu. Agostic Bonding in Pincer Complexes of Ruthenium. *Organometallics* **2000**, *19*, 1734–1739.
- (21) Barthes, C.; Lepetit, C.; Canac, Y.; Duhayon, C.; Zargarian, D.; Chauvin, R. P(CH)P Pincer Rhodium(I) Complexes: The Key Role of Electron-Poor Imidazolophosphine Extremities. *Inorg. Chem.* **2013**, *52*, 48–58.
- (22) Cherry, S. D. T.; Kaminsky, W.; Heinekey, D. M. Structure of a Novel Rhodium Phosphinite Compound: Agostic Interactions as a Model for an Oxidative Addition Intermediate. *Organometallics* **2016**, *35*, 2165–2169.
- (23) Perrin, D. D.; Armarego, W. L. F. *Purification of Laboratory Chemicals*, 3rd ed.; Pergamon: New York, 1988.
- (24) *Bruker computer programs: APEX2, SAINT and SADABS*; Bruker AXS Inc.: Madison, WI, 2015.
- (25) Sheldrick, G. M. Crystal structure refinement with SHELXL. *Acta Crystallogr., Sect. C: Struct. Chem.* **2015**, *A71*, 3–8.
- (26) Spek, A. L. Structure validation in chemical crystallography. *Acta Crystallogr., Sect. D: Biol. Crystallogr.* **2009**, *D65*, 148–155.
- (27) Macrae, C. F.; Edgington, P. R.; McCabe, P.; Pidcock, E.; Shields, G. P.; Taylor, R.; Towler, M.; van de Streek, J. Mercury: visualization and analysis of crystal structures. *J. Appl. Crystallogr.* **2006**, *39*, 453–457.
- (28) Frisch, M. J.; Trucks, G. W.; Schlegel, H. B.; Scuseria, G. E.; Robb, M. A.; Cheeseman, J. R.; Scalmani, G.; Barone, V.; Mennucci, B.; Petersson, G. A.; Nakatsuji, H.; Caricato, M.; Li, X.; Hratchian, H. P.; Izmaylov, A. F.; Bloino, J.; Zheng, G.; Sonnenberg, J. L.; Hada, M.; Ehara, M.; Toyota, K.; Fukuda, R.; Hasegawa, J.; Ishida, M.; Nakajima, T.; Honda, Y.; Kitao, O.; Nakai, H.; Vreven, T.; Montgomery, Jr., J. A.; Peralta, J. E.; Ogliaro, F.; Bearpark, M.; Heyd, J. J.; Brothers, E.; Kudin, K. N.; Staroverov, V. N.; Kobayashi, R.; Normand, J.; Raghavachari, K.; Rendell, A.; Burant, J. C.; Iyengar, S. S.; Tomasi, J.; Cossi, M.; Rega, N.; Millam, J. M.; Klene, M.; Knox, J. E.; Cross, J. B.; Bakken, V.; Adamo, C.; Jaramillo, J.; Gomperts, R.; Stratmann, R. E.; Yazyev, O.; Austin, A. J.; Cammi, R.; Pomelli, C.; Ochterski, J. W.; Martin, R. L.; Morokuma, K.; Zakrzewski, V. G.; Voth, G. A.; Salvador, P.; Dannenberg, J. J.; Dapprich, S.; Daniels, A. D.; Farkas, Ö.; Foresman, J. B.; Ortiz, J. V.; Cioslowski, J.; Fox, D. J., *Gaussian 09*, Revision A.02; Gaussian, Inc.: Wallingford, CT, 2009.
- (29) Hehre, W. J.; Radom, L.; Schleyer, P. v. R.; Pople, J. A. *Ab Initio Molecular Orbital Theory*; John Wiley & Sons, New York, 1986.
- (30) Parr, R. G.; Yang, W. *Density Functional Theory of Atoms and Molecules*; Oxford University Press, New York, 1989.
- (31) Becke, A. D. Density-functional thermochemistry. III. The role of exact exchange. *J. Chem. Phys.* **1993**, *98*, 5648–5652.
- (32) Lee, C.; Yang, W.; Parr, R. G. Development of the Colle-Salvetti correlation-energy formula into a functional of the electron density. *Phys. Rev. B: Condens. Matter Mater. Phys.* **1988**, *37*, 785–789.
- (33) Miehlich, B.; Savin, A.; Stoll, H.; Preuss, H. Results obtained with the correlation energy density functionals of Becke and Lee, Yang and Parr. *Chem. Phys. Lett.* **1989**, *157*, 200–206.
- (34) (a) Haeusermann, U.; Dolg, M.; Stoll, H.; Preuss, H.; Schwerdtfeger, P.; Pitzer, R. M. Accuracy of energy-adjusted quasirelativistic ab initio pseudopotentials. *Mol. Phys.* **1993**, *78*, 1211–1224. (b) Kuechle, W.; Dolg, M.; Stoll, H.; Preuss, H. Energy-adjusted pseudopotentials for the actinides. Parameter sets and test calculations for thorium and thorium monoxide. *J. Chem. Phys.* **1994**, *100*, 7535–7542. (c) Leininger, T.; Nicklass, A.; Stoll, H.; Dolg, M.; Schwerdtfeger, P. The accuracy of the pseudopotential approximation. II. A comparison of various core sizes for indium pseudopotentials in calculations for spectroscopic constants of InH, InF, and InCl. *J. Chem. Phys.* **1996**, *105*, 1052–1059.
- (35) (a) McLean, A. D.; Chandler, G. S. Contracted Gaussian basis sets for molecular calculations. I. Second row atoms,  $Z = 11–18$ . *J. Chem. Phys.* **1980**, *72*, 5639–5648. (b) Krishnan, R.; Binkley, J. S.; Seeger, R.; Pople, J. A. Self-consistent molecular orbital methods. XX. A basis set for correlated wave functions. *J. Chem. Phys.* **1980**, *72*, 650–654. (c) Wachters, A. J. H. Gaussian Basis Set for Molecular Wavefunctions Containing Third-Row Atoms. *J. Chem. Phys.* **1970**, *52*, 1033–1036. (d) Hay, P. J. Gaussian basis sets for molecular calculations - The representation of 3d orbitals in transition-metal atoms. *J. Chem. Phys.* **1977**, *66*, 4377–4384. (e) Raghavachari, K.; Trucks, G. W. Highly correlated systems. Excitation energies of first row transition metals Sc-Cu. *J. Chem. Phys.* **1989**, *91*, 1062–1065. (f) Binning, R. C., Jr.; Curtiss, L. A. Compact contracted basis sets for third-row atoms: Ga–Kr. *J. Comput. Chem.* **1990**, *11*, 1206. (g) McGrath, M. P.; Radom, L. Extension of Gaussian-1 (G1) theory to bromine-containing molecules. *J. Chem. Phys.* **1991**, *94*, 511–516.
- (36) Weinhold, F.; Carpenter, J. E. *The Structure of Small Molecules and Ions*; Plenum, New York, 1988; p 227.
- (37) (a) Wiberg, K. B. Application of the pople-santry-segal CNDO method to the cyclopropylcarbonyl and cyclobutyl cation and to bicyclobutane. *Tetrahedron* **1968**, *24*, 1083–1096. (b) Wiberg indices are electronic parameters related with the electron density in between two atoms, which scale as bond strength indicators. They can be obtained from a Natural Population Analysis.
- (38) Glendening, E. D.; Badenhop, J. K.; Reed, A. E.; Carpenter, J. E.; Bohmann, J. A.; Morales, C. M.; Weinhold, F. *Theoretical Chemistry Institute*; University of Wisconsin, Madison, 2001.
- (39) Portmann, S.; Lüthi, H. P. MOLEKEL: An Interactive Molecular Graphics Tool. *Chimia* **2000**, *54*, 766–770.